

Selected Paper

X-ray Analysis of Excited-State Structures of the Diplatinum Complex Anions in Five Crystals with Different Cations

Nobuhiro Yasuda, Hidehiro Uekusa, and Yuji Ohashi*

Department of Chemistry and Materials Science, Tokyo Institute of Technology, Ookayama, Meguro-ku, Tokyo 152-8551

Received September 24, 2003; E-mail: yohashi@cms.titech.ac.jp

The photo-excited structures of $[Pt_2(pop)_4]^{4-}$ and $[Pt_2(pop)_2(popH)_2]^{2-}$, (pop = diphosphite) in five kinds of complexes were analyzed by X-rays. For the complex with tetrabutylammonium (Bu), tetrapentylammonium (Pn), benzyltriethylammonium (Bzte), or benzyltributylammonium (Bztbu) as a counter cation, the Pt complex anion is attached by two protons and is represented as $[Pt_2(pop)_2(popH)_2]^{2-}$, whereas the anion is $[Pt_2(pop)_4]^{4-}$ for the complex with benzyldimethylphenylammonium (Bzdmp) as a cation. Since the Bu, Pn, and Bzte complexes have two crystal forms, the structures of eight crystals, Bu1, Bu2, Pn1, Pn2, Bzte1, Bzte2, Bztbu, and Bzdmp, were determined by X-ray analysis before irradiation. The five crystals of Bu1, Pn1, Bzte1, Bztbu, and Bzdmp were irradiated with a xenon lamp. The intensity data were collected at the light-on and light-off stages at 173 K for Bu1, Pn1, and Bzdmp crystals and at 103 K for Bzte1 and Bztbu crystals. Each crystal showed the contraction of the unit-cell volume significantly at light-on stage and returns to the original one at light-off stage. The analyzed structures at light-on and light-off stages clearly indicated that the Pt–Pt and Pt–P bond distances became significantly shorter at light-on stage than the corresponding distances at light-off stage. The decreased values for the Pt–Pt and Pt–P distances at the light-on stage are 0.0038(3) and 0.0069(10) Å for Bu1, 0.0081(3) and 0.0053(11) Å for Pn1, 0.0127(5) and 0.0085(14) Å for Bzte1, 0.0031(3) and 0.0019(12) Å for Bztbu, and 0.0019(2) and 0.0033(8) Å for Bzdmp, respectively. The other bond distances in anions and cations are not significantly changed. These structural changes indicate that the excited- and ground-state molecules reach the equilibrium state at the light-on stage; the values are in good agreement with the results observed by spectroscopic methods and theoretical calculation.

It has been believed for a long time that X-ray analysis is applicable only to the stable structures in the crystalline state. However, we have reported a variety of crystalline-state reactions such as photo-racemization[1] and photo-isomerization[2] of cobaloxime complexes, the cyclization reactions[3] and the oxygen insertion reaction,[4] in which the reactant molecules are completely changed to the product molecules with retention of the single crystal form. In the two-step reactions, unstable intermediate structures were observed by X-ray analysis.[5] This indicates that the structures of the reaction intermediates as well as the reactant and product molecules can be observed by X-ray analysis in the crystalline-state reactions.

Recently several structures of unstable species, such as unstable structures of photochromic crystals,[6] intermediate nitrosyl–metal complexes,[7] and photoproduced radical pairs,[8] triplet carbenes,[9] and triplet nitrenes,[10] have been analyzed by X-rays. These structure analyses suggest that the unstable structures can be observed by X-ray analysis at low temperatures less than 100 K, although the produced unstable species were less than 5–10% concentration in the original crystal.

Moreover, several excited-state structures have been analyzed using synchrotron radiation. A combination of excitation by laser light and Laue diffraction method using polychromatic synchrotron radiation made it possible to obtain the excited-state structure. A picosecond diffraction study of *N*,*N*-dimethylaminobenzonitrile has shown the torsional distortion at the excited state.[11] The reaction processes in protein molecules have been reported.[12] Although the Laue method is very attractive to collect the diffraction data in a very short time (within a nano or micro second), it seems difficult to obtain the precise structure. Coppens et al. reported the excited-state structure of a Pt complex anion, $[Pt_2(pop)_3(popH)]^{3-}$, where pop is diphosphite, $(H_2P_2O_5)^{2-}$.[13] They proposed the stroboscopic technique, in which the molecules in a crystal were repeatedly excited by a pulsed laser and the structural change was probed for a period of microseconds immediately after the excitation by pulsed monochromatic X-ray of synchrotron radiation. The above two time-resolved diffraction techniques are very useful methods to analyze the transient irreversible structural changes. However, it is not necessary to use such techniques for the observation of the unstable structure with reversible changes, such as the excited-state structure, because the summation of the diffraction by X-ray pulses is essentially the same as the structure analysis by continuous monochromatic X-ray diffraction if we can assume that the excited structure does not change to the other transient ones and that there are only two structures, composed of the ground and excited states, in the irradiated crystal. The diffraction should be brought about by the periodic structure composed of the equilibrium structure between the ground-state and excited-state molecules. If the concentration of the excited molecules exceeds the threshold value in the equilibrium structure, the structure of the excited molecule can be analyzed using the diffraction data at light-on stage (during irradiation). The concentration or occupancy factor of excited molecules, which is the most important factor, depends mainly on the wavelength of the incident light. The light with

Published on the web May 6, 2004; DOI 10.1246/bcsj.77.933

the wavelength of absorption maximum may excite only the surface molecules and it would not be able to excite the molecules in the inner part of the crystal. Although the light with longer wavelength can penetrate into the crystal more effectively, the number of photons absorbed would be small. Because the data collection time is not limited for the reversible photoreactions, the light with longer continuous wavelengths seems to be better than the stronger pulsed-light with the wavelength of absorption maximum.

We intended to develop a conventional photo-crystallographic method utilizing the irradiation with continuous wavelengths and continuous X-rays with monochromatic wavelength to observe the excited-state molecules. The crystal would be in the equilibrium state between the ground and excited states when it was photoirradiated and kept at low temperatures. The light with longer wavelengths than the absorption maximum was selected to allow the light to penetrate effectively into the crystal. If the concentration of the excited molecules exceeds the threshold value (≈5%) at the equilibrium condition, the reversible structural change, no matter how quickly it occurs, should be observed by the method.

Kaizu et al. reported that the powder pattern of the Pt complex, $[N(C_4H_9)_4]_4[Pt_2(pop)_4]$, shifted reversibly to its higher diffraction angle when the powdered sample was irradiated with a xenon lamp at low temperatures.[14] This experiment indicated that the structural change of the Pt complex in the excited state is large and so the concentration of the excited molecules probably exceeds the threshold value. Such an observation of the reversible lattice change at low temperatures is very important to check the possibility whether the excited structure can be observed by X-ray analysis or not.

Some preliminary results have been reported using the Pt complex, $[Pt_2(pop)_2(popH)_2]^{2-}$, with the tetrabutylammonium, Bu1[15] and tetrapentylammonium cations, Pn1.[16] The present paper reports the structures of the polymorphic forms of the Bu1 and Pn1 complexes, (Bu2 and Pn2, respectively), and the additional complexes with the benzyltriethylammonium (Bzte1 and Bzte2), benzyltributylammonium (Bztbu), and benzyldimethylphenylammonium (Bzdmp) cations, as shown in Scheme 1, and compares the excited structures of the Pt complex anions in the five complex crystals: Bu1, Pn1, Bzte1, Bztbu, and Bzdmp. The reason why such alkylammonium ions are used for the counter cations is to loosen the crystal packing around the Pt complex anion and to make the complex crystal transparent to the exciting light except for the Pt complex anion.

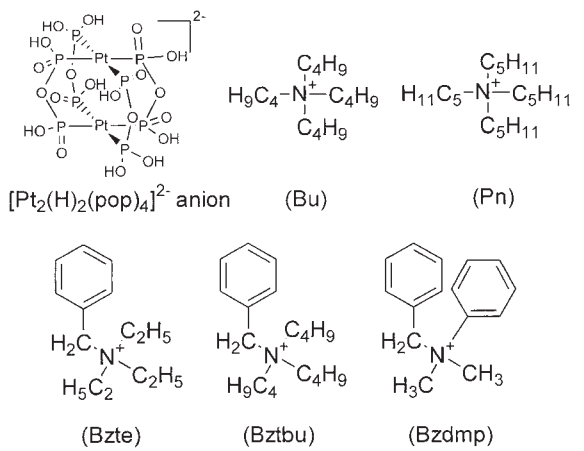

Scheme 1. Structures of Pt complex anion and Bu, Pn, Bzte, Bztbu, and Bzdmp cations.

Experimental

Preparation of the Complex Crystals. The Pt complexes with various cations were synthesized by the method for $[N(C_4H_9)_4]_4[Pt_2(pop)_4]$ complex reported previously.[17] The crude products were obtained under nitrogen atmosphere. The yellowish green crystals suitable for X-ray measurements were obtained from methanol solutions under ether atmosphere. The preliminary X-ray analyses of the crystals of the five complexes, except for Bzdmp, revealed that there are only two cations per one Pt complex anion and that two of the eight P=O bonds have nearly the same length as the P–OH bond. This indicates that two protons are attached to the P=O groups of the Pt complex anion and that the Pt complex can be represented by $[Pt_2(pop)_2(popH)_2]^{2-}$. For the Bzdmp complex, one Pt complex has four cations and the eight P=O bonds have nearly the same lengths. This means that the anion can be represented by $[Pt_2(pop)_4]^{4-}$.

Polymorphism of the Complex Crystals. The preliminary X-ray analyses indicated that polymorphic crystals were found among the Bu, Pn, and Bzte complexes in the same batch. For the Bu complex, the plate crystal, Bu1, has no solvent molecule, whereas the needle crystal, Bu2, includes one methanol molecule in the asymmetric unit. For the Pn complex, the appearances of the two crystal forms are very similar to each other and it is impossible to distinguish the two forms under the microscope. The preliminary X-ray measurements revealed that, although the unit-cell dimensions are different, both of them have the same space group and no solvent molecules. The only difference between the two polymorphs is the relative orientation of the $[Pt_2(pop)_2(popH)_2]^{2-}$ anion to the neighboring ones. This causes the disordered structure of one of the cations. The Pn2 crystal was easily converted to Pn1 when it was ground in a mortar.

For the Bzte complex, both of the crystal forms are plate-like. One crystal form, Bzte1, has a twin structure, but each component of the twin can be separated with a blade under the polarized microscope. The preliminary X-ray analysis indicated that Bzte1 has no solvent molecule, whereas the other crystal, Bzte2, has a methanol molecule in the asymmetric unit. The crystal of Bzte2 was gradually decomposed due to the elimination of methanol solvent.

Crystal data of Bu2, Pn2, and Bzte2 are summarized in Table 1. Crystal data of Bu1, Pn1, Bzte1, Bztbu, and Bzdmp are given in Table 2.

Selection of the Light Source. The absorption spectra of an aqueous solution of the Pn complex were measured with a vis/UV spectrometer (Shimadzu UV-3100); they are shown in Fig. 1. The absorption spectra of $[Pt_2(pop)_2(popH)_2]^{2-}$ anion are characterized at about 360 and 450 nm; these values are in good agreement with those of the $[Pt_2(pop)_4]^{4-}$ anion.[18] Because the light with the longer wavelength can penetrate into the crystal more deeply, the range of the wavelength for the excitation light was selected from 400 to 550 nm. In order to satisfy the conditions, a xenon lamp with filters (HOYA blue filter B460 and long pass filter L39, $\lambda = 470 \pm 80$ nm) was used. The light was brought to the crystal on the diffractometer using a glass fiber. Figure 2 shows the color change of the Pn1 crystal at the light-off and light-on stages.

Table 1. Crystal Data and Experimental Details of Bu2, Pn2, and Bzte2

	Bu2	Pn2	Bzte2
Formula	$C_{32}H_{82}N_2O_{20}P_8Pt_2/CH_3OH$	$C_{40}H_{98}N_2O_{20}P_8Pt_2$	$C_{26}H_{54}N_2O_{20}P_8Pt_2/CH_3OH$
Formula weight	1484.98	1565.14	1384.69
Temperature/K	103(2)	223(2)	103(2)
Wavelength/Å	0.71069	0.71073	0.71073
Crystal size/mm^3	0.40 × 0.06 × 0.06	0.30 × 0.07 × 0.05	0.32 × 0.20 × 0.03
Crystal system	Orthorhombic	Triclinic	Orthorhombic
Space group	$P2_12_12_1$	$P\bar{1}$	$Pna2_1$
Z	4	2	4
a/Å	9.4870(3)	9.45410(10)	20.42330(10)
b/Å	20.3145(7)	16.9411(2)	21.6230(2)
c/Å	27.7153(13)	20.68590(10)	10.10650(10)
α/°	90	91.9743(8)	90
β/°	90	98.3843(3)	90
γ/°	90	104.2355(9)	90
V/Å^3	5341.4(4)	3168.50(5)	4463.16(6)
D_{calcd}/Mg m^{-3}	1.847	1.641	2.061
μ/mm^{-1}	5.544	4.677	6.627
θ range/°	2.27 to 27.48	1.24 to 27.48	1.99 to 27.48
Reflections collected/unique	35286/11038	22594/14268	30527/9974
R_{int}	0.0479	0.0293	0.0557
Completeness to $\theta = 27.48°$	0.939	0.982	0.998
Data/restraints/parameters	11038/0/593	14268/4/669	9974/1/546
$R_1[I > 2\sigma(I)]$	0.0350	0.0343	0.0291
No. of $I > 2\sigma(I)$ (refs.)	10525	12040	9538
Largest diff. peak (e Å^{-3})	1.073	1.631	1.622
Largest diff. hole (e Å^{-3})	−1.368	−1.468	−1.954

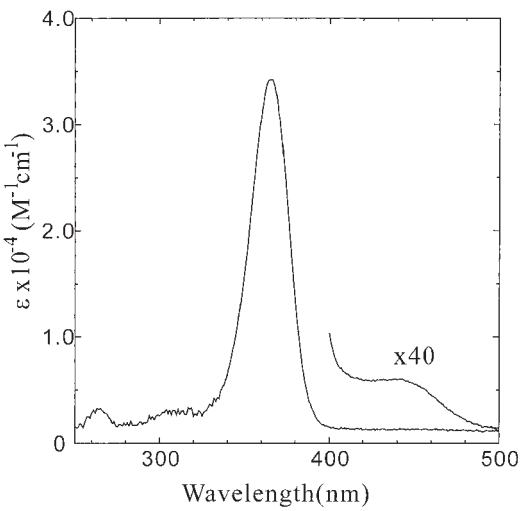

Fig. 1. Absorption spectra of an aqueous solution of the Pn complex.

Diffraction from the Powdered Sample before and during the Photoirradiation. In order to confirm the decrease in cell volume by photoirradiation as observed for the $[N(C_4H_9)_4][Pt_2(pop)_4]$ crystal,[14] the powder diffraction pattern of Pn1 was measured at the BL02B2 beam line of SPring-8. The powdered sample was filled in a glass capillary (0.3 mm diameter) and was mounted on a Debye-Scherrer camera with the diameter of 28.65 cm. The wavelength was 1.08 Å and measured $2\theta_{min}$ and $2\theta_{max}$ were 2.5 and 75°, respectively. The sample was cooled to 173 K with a cold-nitrogen-gas stream and was irradiated with the light described above.

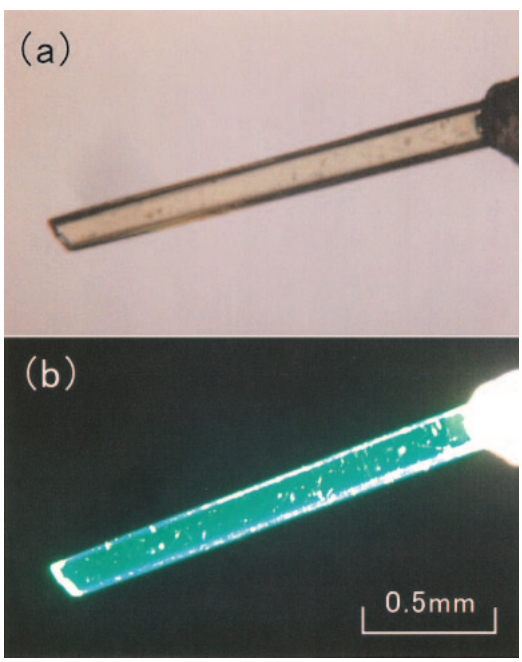

Fig. 2. Color change of the Pn1 crystal under the microscope; (a) at the light-off stage and (b) at the light-on stage.

Crystal Structure Analyses before and during Irradiation. All the intensity data of eight crystals: Bu1, Bu2, Pn1, Pn2, Bzte1, Bzte2, Bztbu, and Bzdmp, were collected before the photoirradiation, using a Bruker Smart-CCD diffractometer with the rotating-anode X-ray generator. Since the crystals of Bu2 and Bzte2 have

Table 2. Crystal Data and Experimental Details of Bu1, Pn1, Bzte1, Bztbu, and Bzdmp at Light-Off and Light-On Stages

	Bu1-OFF	Bu1-ON	Pn1-OFF	Pn1-ON	Bztel-OFF	Bztel-ON	Bztbu-OFF	Bztbu-ON	Bzdmp-OFF	Bzdmp-ON
Formula	$C_{32}H_{82}N_2O_{20}P_8Pt_2$		$C_{40}H_{98}N_2O_{20}P_8Pt_2$		$C_{26}H_{54}N_2O_{20}P_8Pt_2$		$C_{38}H_{78}N_2O_{20}P_8Pt_2$		$C_{31}H_{44}N_2O_{11}P_4Pt$	
Formula weight	1452.94		1565.14		1352.65		1520.96		939.65	
Temperature/K	173(2)		173(2)		103(2)		103(2)		173(2)	
Wavelength/Å	0.71073		0.71073		0.71073		0.71073		0.71073	
Crystal size/mm^3	$0.12 \times 0.10 \times 0.10$		$0.40 \times 0.05 \times 0.02$		$0.15 \times 0.08 \times 0.02$		$0.18 \times 0.08 \times 0.05$		$0.20 \times 0.17 \times 0.10$	
Crystal system	Triclinic		Triclinic		Triclinic		Triclinic		Monoclinic	
Space group	$P\bar{1}$		$P\bar{1}$		$P\bar{1}$		$P\bar{1}$		$P2_1/n$	
Z	1		2		2		2		4	
a/Å	12.40780(10)	12.3768(3)	9.69650(10)	9.6758(3)	11.8647(4)	11.8488(3)	9.5229(3)	9.5199(2)	13.74370(10)	13.73350(10)
b/Å	12.4747(2)	12.4443(3)	17.2492(3)	17.2106(6)	12.5661(4)	12.5275(4)	14.3046(5)	14.2924(4)	12.9901(2)	12.9877(2)
c/Å	9.64630(10)	9.6268(2)	18.7278(2)	18.6822(6)	14.7700(5)	14.7425(5)	20.8753(7)	20.8590(6)	21.04720(10)	21.03340(10)
α/°	96.0435(8)	95.9963(6)	93.6649(4)	93.6675(8)	89.3129(9)	89.3304(6)	90.4165(3)	90.4352(7)	90	90
β/°	91.3580(8)	91.3709(8)	90.9346(8)	90.9035(4)	88.0813(6)	87.9796(12)	97.3252(8)	97.3120(7)	105.9300(10)	105.9380(10)
γ/°	116.8715(3)	116.7862(8)	102.8259(7)	102.8002(8)	73.3677(9)	73.3187(7)	106.8507(8)	106.8467(5)	90	90
V/Å^3	1320.18(3)	1312.16(5)	3046.45(7)	3026.12(17)	2108.78(12)	2094.92(11)	2696.42(16)	2691.27(12)	3613.30(6)	3607.44(6)
D_{calcd}/Mg m^{-3}	1.828	1.839	1.706	1.718	2.130	2.144	1.873	1.877	1.727	1.730
μ/mm^{-1}	5.604	5.639	4.864	4.897	7.009	7.055	5.493	5.503	4.120	4.127
θ range/°	1.85 to 27.48	1.85 to 27.48	1.09 to 27.48	1.09 to 27.48	1.38 to 27.48	1.38 to 27.48	1.49 to 27.48	1.49 to 27.48	2.01 to 27.48	1.86 to 27.48
Reflections collected/unique	9357/5883	9268/5821	21788/13755	21211/13429	15069/9552	9429/7550	13248/9927	13212/9900	25314/8275	25234/8264
R_{int}	0.0281	0.0257	0.0325	0.0325	0.0346	0.0385	0.0271	0.0288	0.0340	0.0347
Completeness to $\theta = 27.48°$	0.971	0.966	0.984	0.967	0.987	0.785	0.802	0.802	0.998	0.998
Data/restraints/parameters	5883/0/289	5821/0/289	13755/0/670	13429/0/673	9552/0/553	7550/0/541	9927/0/644	9900/0/655	8275/0/436	8264/0/436
$R_1[I > 2\sigma(I)]$	0.0284	0.0274	0.0333	0.0335	0.0332	0.0380	0.0336	0.0353	0.0262	0.0274
No. of $I > 2\sigma(I)$ (refs.)	5407	5406	11246	11009	8039	6084	8969	8893	7561	7529
Largest diff. peak (e Å^{-3})	1.604	1.480	1.372	1.363	2.561	1.603	1.831	2.095	1.155	1.417
Largest diff. hole (e Å^{-3})	−1.652	−1.385	−1.427	−1.453	−2.490	−1.387	−1.515	−1.421	−1.524	−1.482

solvent molecules and Pn2 has a disordered structure, these three crystals were not used for the photo-excitation experiment.

The intensity data of Bu1 were collected in the dark (light-off) at 173 K, since the cell change was the largest at 173 K, as shown in the preliminary work.[16] Then the light was turned on and the intensity data were collected under the same conditions (light-on) as those at the light-off stage. The intensity data of the other four crystals, Pn1, Bzte1, Bztbu, and Bzdmp, were collected at the light-off and light-on stages under the same conditions as those for Bu1, except that the temperature was changed to 103 K for the Bzte1 and Bztbu crystals. Crystal data at light-on stage are given in Table 2.

Each structure was solved by the direct method (SHELXS-97)[19] and refined by the full-matrix least-squares method (SHELXL-97).[20] All the non-hydrogen atoms were found in the difference Fourier map. All hydrogen atoms of the cations were located geometrically. Some hydrogen atoms of the Pt complex anion were located in a difference Fourier map. The other ones were located from the geometrical calculations considering the P–O bond distances and the intermolecular O···O hydrogen bonds. All the non-hydrogen atoms were refined anisotropically and the hydrogen atoms were refined isotropically.

The crystal data and atomic parameters have been deposited at the CCDC, 12 Union Road, Cambridge CB2 1EZ, UK and copies can be obtained on request, free of charge, by quoting the publication citation and the deposition numbers 226198–226210.

Results

Two Crystal Forms of Bu. Two crystal forms, Bu1 and Bu2, were produced in the same batch. The Bu2 crystal form has one solvent methanol molecule per Pt complex. The crystal structure of Bu1 is shown in Fig. 3. Each Pt complex lie on a center of symmetry and the Pt complexes are connected with the neighboring complexes by two O–H···O hydrogen bonds and make a linear chain along the *c* axis. The O···O distances and O–H···O angles of the hydrogen bonds are listed in Table 3.

The crystal structure of Bu2 is shown in Fig. 4. A similar hydrogen bond chain connects the Pt complexes along the *a* axis.

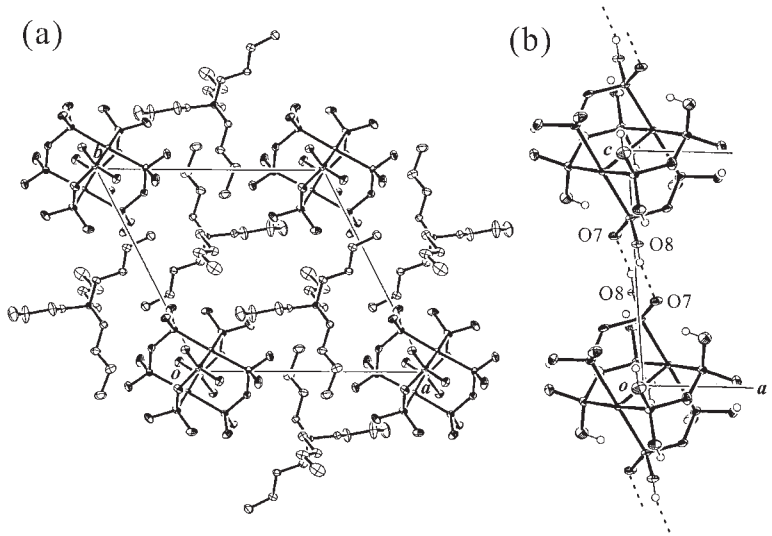

Fig. 3. (a) Crystal structure of Bu1 viewed along the *c* axis and (b) the hydrogen bonding chain along the *c* axis.

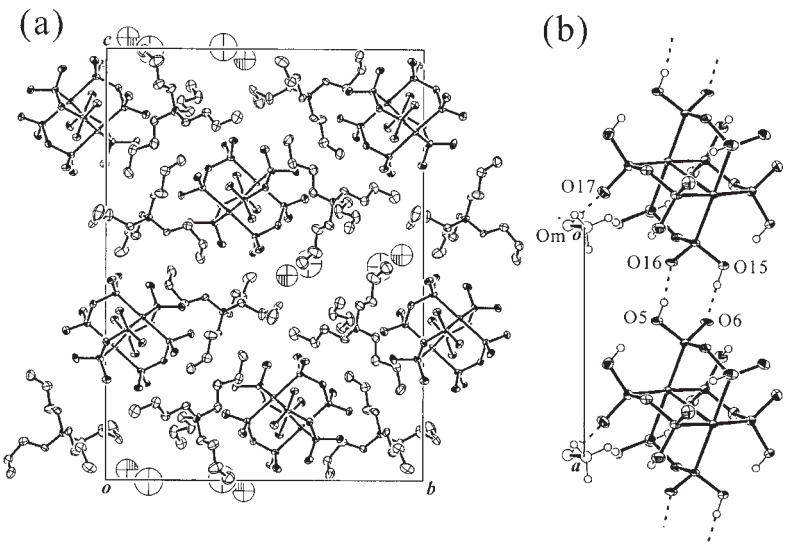

Fig. 4. (a) Crystal structure of Bu2 viewed along the *a* axis and (b) the hydrogen bonding chain along the *a* axis.

Table 3. Hydrogen Bond Lengths (Å) and Angles (°) in the Bu1, Pn1, Bzte1, Bztbu, and Bzdmp Crystals at Light-Off and Light-On Stages

	D–H···A	D–H/Å	H···A/Å	D···A/Å	D–H···A/°
Bu1-OFF	O8–H8···O7^{i}	0.84	1.72	2.519(4)	157.3
Bu1-ON	O7–H7···O8^{i}	0.84	1.78	2.510(4)	144.8
Bu2	OM–HM0···O17	0.84	2.09	2.93(2)	172.8
	O5–H5···O16^{ii}	0.84	1.69	2.522(7)	169.6
	O15–H15···O6^{iii}	0.84	1.66	2.492(7)	170.8
Pn1-OFF	O8–H8···O7^{iv}	0.86(6)	1.77(6)	2.627(4)	175(6)
	O14–H14···O13^{v}	0.84	1.70	2.537(4)	171.1
Pn1-ON	O8–H8···O7^{iv}	0.79(6)	1.83(6)	2.620(5)	171(6)
	O14–H14···O13^{v}	0.93(6)	1.68(6)	2.526(4)	150(6)
Pn2	O1–H1···O2^{v}	0.83	1.71	2.532(4)	170.3
	O15–H15···O16^{vi}	1.05(6)	1.48(6)	2.506(4)	162(5)
Bztel-OFF	O2–H2···O17^{vii}	1.20(6)	1.34(7)	2.460(5)	152(6)
	O3–H3···O18^{vii}	0.84(6)	2.06(6)	2.763(5)	141(6)
	O12–H12···O7	0.80(8)	1.74(8)	2.495(6)	158(7)
	O13–H13···O8	0.96(7)	1.59(8)	2.553(6)	173(6)
Bztel-ON	O3–H3···O18^{vii}	0.77(9)	2.42(9)	2.785(8)	111(8)
	O12–H12···O7	0.86(9)	1.75(9)	2.498(7)	145(9)
	O13–H13···O8	0.84	1.81	2.557(7)	146.9
	O17–H17···O2^{viii}	0.84	1.62	2.459(7)	176.8
Bzte2	O7–H7···O20^{vii}	0.84	1.66	2.468(5)	159.3
	O14–H14···O1^{ix}	0.84	1.74	2.491(6)	147.3
	O50–H50···O6	0.87(11)	2.07(11)	2.926(7)	167(11)
Bztbu-OFF	O7–H7···O8^{i}	0.84	1.72	2.533(4)	163.6
	O17–H17···O18^{x}	1.12(5)	1.38(5)	2.493(4)	171(5)
Bztbu-ON	O7–H7···O8^{i}	1.12(6)	1.40(6)	2.521(5)	175(6)
	O17–H17···O18^{x}	1.14(6)	1.35(6)	2.489(4)	171(6)
Bzdmp-OFF	O50–H50···O1	0.85	1.96	2.813(3)	173.9
Bzdmp-ON	O50–H50···O1	0.85	1.96	2.815(4)	173.9

Symmetry operations: i) $-x, -y, 1-z$; ii) $1+x, y, z$; iii) $-1+x, y, z$; iv) $-x, 2-y, -z$; v) $1-x, 1-y, 1-z$; vi) $1-x, -y, -z$; vii) $x, y, -1+z$; viii) $x, y, 1+z$; ix) $x+0.5, -y+0.5, z$; x) $-x, 1-y, -z$.

The solvent methanol molecule makes a hydrogen bond with the Pt complex. The hydrogen bond distances and angles are also given in Table 3.

Two Crystal Forms of Pn. Two crystal forms were obtained in the same batch, Pn1 and Pn2. Neither of them have any solvent molecules. The crystal structures of Pn1 and Pn2 are shown in Figs. 5 and 6, respectively. Either crystal has two crystallographically independent Pt complexes that occupy the different centers of symmetry. The Pt complexes are connected with the neighboring complexes by the O–H···O hydrogen bonds to form a linear chain, as observed in Bu1 crystal. The chain is extended along the *a* axis in each crystal. In Pn2, one alkyl chain of the cations is disordered, although all the alkyl chains are ordered in Pn1. This is due to the void space that is made by the slight orientation change of the Pt complex anions in the Pn2 crystal. The hydrogen bond distances and angles are listed in Table 3.

Two Crystal Forms of Bzte. There are two crystal forms for the Bzte complexes, Bzte1 and Bzte2. Their crystal structures are shown in Figs. 7 and 8, respectively. The Bzte1 crystal has no crystal solvent and the two Pt complexes occupy the different centers of symmetry, whereas the Bzte2 crystal has one methanol molecule as a crystal solvent, which is attached to the Pt complex. In each crystal, the Pt complexes are connected with the O–H···O hydrogen bonds to form a two-dimensional sheet. The hydrogen bond distances and angles are listed in Table 3.

Crystal Structure of Bztbu. There is only one crystal form for the Bztbu complex, whose crystal structure is shown in Fig. 9. The two crystallographically independent Pt complexes occupy the different inversion centers. The Pt complexes are connected with the neighboring Pt complexes by a pair of O–H···O hydrogen bonds to form a chain along the *a* axis. The hydrogen bond distances and angles are listed in Table 3.

Crystal Structure of Bzdmp. There is only one crystal form for the Bzdmp complex. The crystal structure is shown in Fig. 10. The Pt complex has a different structure from those of the above crystals, since no proton is attached to the pop moieties. Therefore, the Pt complex is written as $[Pt_2(pop)_4]^{4-}$ and there are four benzyldimethylphenylammonium cations per one Pt complex. The Pt complex is not hydrogen bonded with the neighboring Pt complex anions and is isolated from the other Pt complexes. The two solvent methanol molecules are connected with the Pt complex by the O–H···O hydrogen bonds. The hydrogen bond distances and angles are listed in Table 3. The isolated structure is probably closely related to the no-proton attached anion.

Molecular Structures of the Pt Complexes. The molecular structure of the Pt complex anion in Bu1 with the atomic numbering is shown in Fig. 11. The Pt complexes in the other

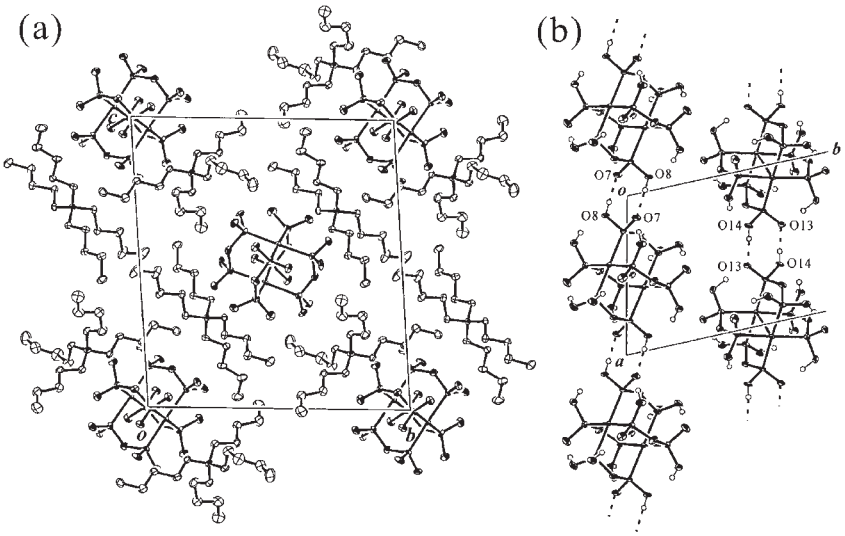

Fig. 5. (a) Crystal structure of Pn1 viewed along the *a* axis and (b) the two crystallographically independent hydrogen bonding chains along the *a* axis.

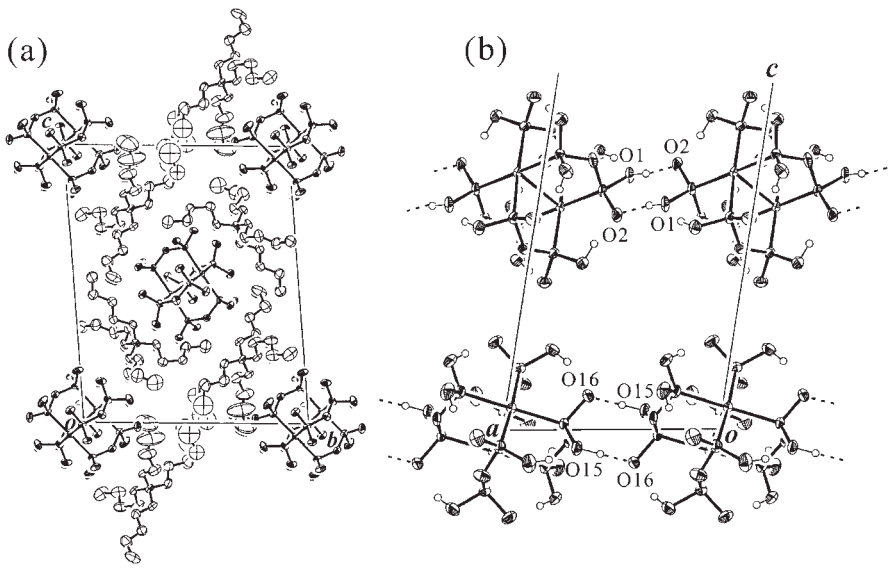

Fig. 6. (a) Crystal structure of Pn2 viewed along the *a* axis and (b) the two hydrogen bonding chains along the *a* axis.

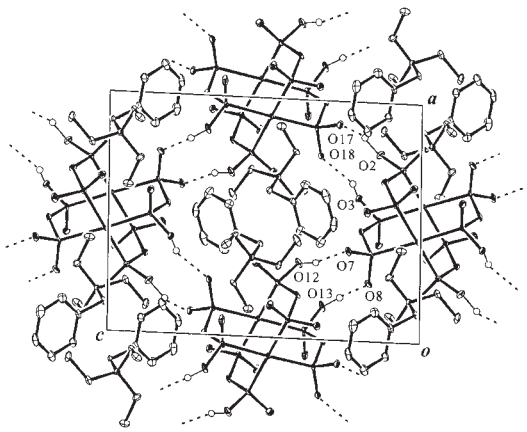

Fig. 7. Crystal structure of Bzte1 viewed along the *b* axis and the hydrogen bonding sheet normal to the *b* axis.

crystals are in good agreement with that in Bu1 except for the Bzdmp complex. The bond distances in the eight Pt complexes before irradiation are listed in Table 4. The bond distances of P–OH are significantly longer than those of P=O. This clearly indicates that there are five P–OH bonds and three P=O bonds among the eight independent P–O bonds in the Pt complexes, except for the Bzdmp complex in which there are four P–OH and P=O bonds. This means two protons are attached to the two diphosphites of the Pt complex anions and the Pt complex anion is represented as $[Pt_2(H_2P_2O_5)_2(H_3P_2O_5)_2]^{2-}$ for the crystals of Bu, Pn, Bzte, and Bztbu. On the other hand, the Pt complex anion in Bzdmp crystal is represented as $[Pt_2(H_2P_2O_5)_4]^{4-}$. The bond distances and angles of cations are normal; they are deposited in the supplementary materials with the bond angles of the Pt complex anions and solvent molecules.

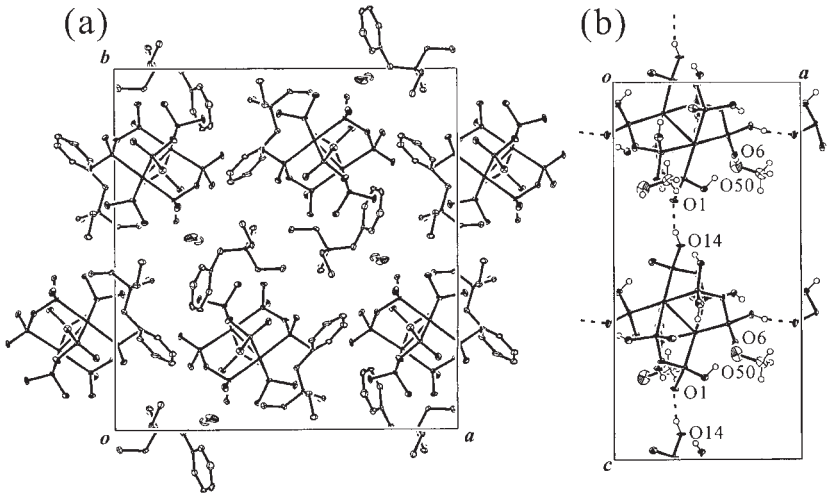

Fig. 8. (a) Crystal structure of Bzte2 viewed along the *c* axis and (b) the hydrogen bonding chain along the *c* axis.

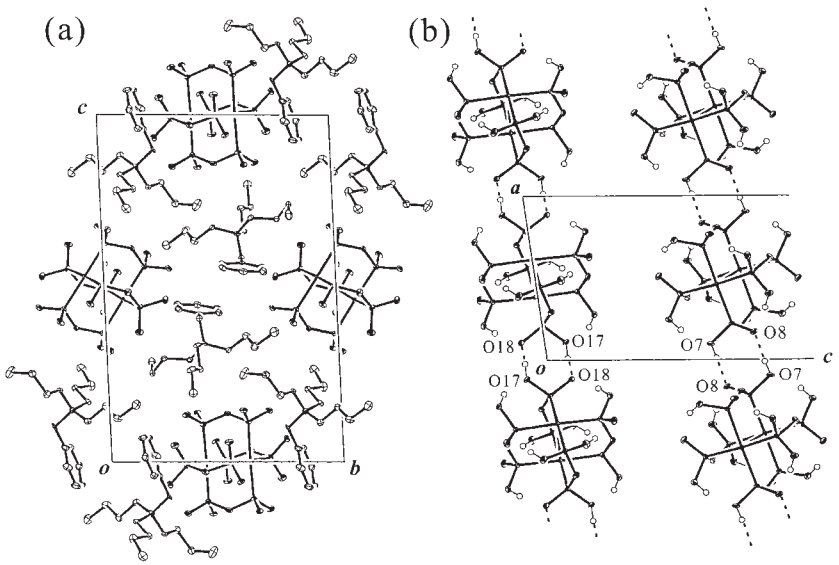

Fig. 9. (a) Crystal structure of Bztbu viewed along the *a* axis and (b) the two hydrogen bonding chains along the *a* axis.

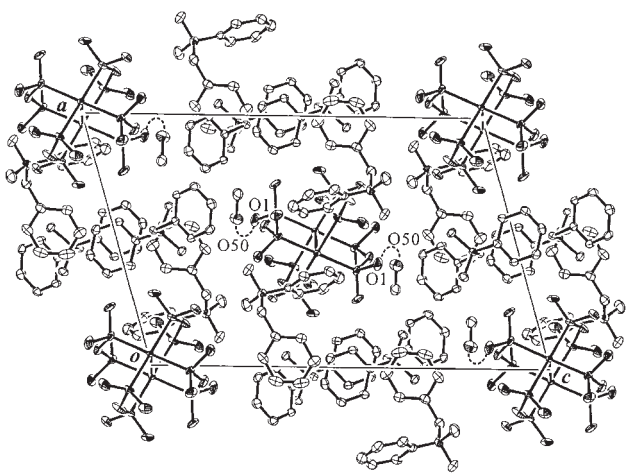

Fig. 10. Crystal structure of Bzdmp viewed along the *b* axis.

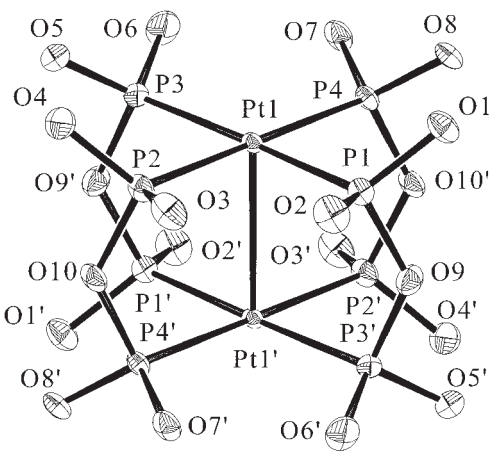

Fig. 11. Molecular structure of the Pt complex anion in Bu1 with the atomic numbering.

Table 4. Bond Lengths (Å) of the Pt Complex Anions with Their Estimated Standard Deviations in Eight Crystals of Bu1, Pn1, Bzte1, Bztbu, Bzdmp, Bu2, Pn2, and Bzte2

Bu1-OFF						Bzdmp-OFF					
Pt1–Pt1	2.9419(3)	P2–O3	1.532(3)	P3–O6	1.589(3)	Pt1–Pt1	2.9203(2)	P1–O1	1.518(3)	P3–O6	1.572(3)
		P3–O5	1.509(3)	P4–O8	1.554(3)			P2–O3	1.522(3)	P4–O8	1.584(3)
Pt1–P1	2.3291(10)	P4–O7	1.565(3)	P1–O9	1.623(3)	Pt1–P1	2.3323(8)	P3–O5	1.530(3)	P1–O9	1.640(3)
Pt1–P2	2.3282(10)	P1–O1	1.584(3)	P2–O10	1.639(3)	Pt1–P2	2.3415(8)	P4–O7	1.517(3)	P2–O10	1.634(3)
Pt1–P3	2.3472(10)	P1–O2	1.523(3)	P3–O9	1.644(3)	Pt1–P3	2.3336(8)	P1–O2	1.582(3)	P3–O9	1.640(2)
Pt1–P4	2.3308(10)	P2–O4	1.565(3)	P4–O10	1.621(3)	Pt1–P4	2.3367(8)	P2–O4	1.575(3)	P4–O10	1.636(3)
Pn1-OFF						Bu2					
Pt1–Pt1	2.9542(3)	P1–O2	1.514(3)	P6–O14	1.577(3)	Pt1–Pt2	2.9233(4)	P1–O6	1.536(5)	P5–O14	1.536(6)
Pt2–Pt2	2.9387(3)	P3–O5	1.506(4)	P7–O15	1.591(3)			P3–O10	1.519(5)	P6–O15	1.581(5)
		P4–O7	1.533(3)	P8–O17	1.539(4)	Pt1–P1	2.3054(19)	P4–O11	1.506(5)	P7–O20	1.569(6)
Pt1–P1	2.3224(12)	P5–O11	1.520(3)	P8–O18	1.544(3)	Pt1–P3	2.3269(19)	P6–O16	1.523(5)	P8–O18	1.563(6)
Pt1–P2	2.3263(12)	P6–O13	1.524(3)	P1–O9	1.620(3)	Pt1–P5	2.3141(19)	P7–O17	1.512(6)	P1–O1	1.617(5)
Pt1–P3	2.3319(12)	P7–O16	1.512(3)	P2–O10	1.634(3)	Pt1–P7	2.3137(19)	P8–O19	1.517(6)	P2–O1	1.624(5)
Pt1–P4	2.3367(11)	P1–O1	1.579(4)	P3–O9	1.629(3)	Pt2–P2	2.310(2)	P1–O5	1.565(5)	P3–O2	1.624(5)
Pt2–P5	2.3257(11)	P2–O3	1.523(4)	P4–O10	1.621(3)	Pt2–P4	2.3206(19)	P2–O7	1.546(5)	P4–O2	1.628(5)
Pt2–P6	2.3154(11)	P2–O4	1.544(4)	P5–O19	1.628(4)	Pt2–P6	2.3052(19)	P2–O8	1.529(6)	P5–O3	1.619(5)
Pt2–P7	2.3274(11)	P3–O6	1.563(4)	P6–O20	1.621(4)	Pt2–P8	2.3144(19)	P3–O9	1.563(6)	P6–O3	1.625(5)
Pt2–P8	2.3262(11)	P4–O8	1.580(4)	P7–O19	1.625(4)			P4–O12	1.577(5)	P7–O4	1.626(5)
		P5–O12	1.574(4)	P8–O20	1.639(4)			P5–O13	1.554(6)	P8–O4	1.630(5)
Bztel-OFF						Pn2					
Pt1–Pt1	2.9657(3)	P3–O5	1.526(4)	P6–O13	1.559(4)	Pt1–Pt1	2.9468(3)	P1–O2	1.527(3)	P5–O12	1.565(4)
Pt2–Pt2	2.9794(4)	P4–O7	1.542(4)	P6–O14	1.549(4)	Pt2–Pt2	2.9657(3)	P2–O4	1.525(3)	P6–O14	1.573(4)
		P4–O8	1.536(4)	P7–O16	1.579(4)			P4–O7	1.514(3)	P7–O15	1.556(4)
Pt1–P1	2.3304(13)	P5–O11	1.554(4)	P8–O18	1.531(4)	Pt1–P1	2.3206(11)	P6–O13	1.513(4)	P8–O17	1.591(4)
Pt1–P2	2.3369(13)	P7–O15	1.518(4)	P1–O9	1.635(4)	Pt1–P2	2.3382(11)	P7–O16	1.569(3)	P1–O9	1.636(3)
Pt1–P3	2.3327(13)	P8–O17	1.550(4)	P2–O10	1.623(4)	Pt1–P3	2.3271(11)	P8–O18	1.526(4)	P2–O10	1.638(3)
Pt1–P4	2.3412(13)	P1–O1	1.575(4)	P3–O9	1.638(3)	Pt1–P4	2.3299(11)	P1–O1	1.586(3)	P3–O9	1.642(3)
Pt2–P5	2.3389(13)	P1–O2	1.536(4)	P4–O10	1.654(4)	Pt2–P5	2.3267(11)	P2–O3	1.579(3)	P4–O10	1.633(3)
Pt2–P6	2.3458(13)	P2–O3	1.577(4)	P5–O19	1.632(4)	Pt2–P6	2.3325(12)	P3–O5	1.550(4)	P5–O19	1.634(3)
Pt2–P7	2.3359(13)	P2–O4	1.543(4)	P6–O20	1.629(4)	Pt2–P7	2.3244(11)	P3–O6	1.537(4)	P6–O20	1.642(4)
Pt2–P8	2.3370(13)	P3–O6	1.583(4)	P7–O19	1.646(4)	Pt2–P8	2.3174(12)	P4–O8	1.586(3)	P7–O19	1.621(3)
		P5–O12	1.546(4)	P8–O20	1.653(4)			P5–O11	1.532(4)	P8–O20	1.619(4)
Bztbu-OFF						Bzte2					
Pt1–Pt1	2.9457(3)	P2–O3	1.539(4)	P6–O14	1.532(4)	Pt1–Pt2	2.9425(3)	P1–O1	1.516(4)	P6–O14	1.568(4)
Pt2–Pt2	2.9330(3)	P3–O5	1.514(3)	P6–O13	1.543(4)			P2–O5	1.521(4)	P7–O16	1.530(4)
		P4–O8	1.533(3)	P7–O16	1.579(3)	Pt1–P1	2.3369(15)	P3–O6	1.517(4)	P7–O17	1.576(4)
Pt1–P1	2.3271(12)	P5–O12	1.519(4)	P8–O17	1.576(3)	Pt1–P3	2.3400(14)	P5–O12	1.529(4)	P8–O19	1.560(4)
Pt1–P2	2.3337(11)	P7–O15	1.519(4)	P1–O9	1.626(3)	Pt1–P5	2.3190(15)	P6–O15	1.508(4)	P1–O3	1.655(4)
Pt1–P3	2.3301(12)	P8–O18	1.537(4)	P2–O10	1.630(3)	Pt1–P7	2.3292(15)	P8–O20	1.540(4)	P2–O3	1.609(4)
Pt1–P4	2.3198(11)	P1–O2	1.529(4)	P3–O9	1.632(4)	Pt2–P2	2.3192(15)	P1–O2	1.560(4)	P3–O8	1.670(4)
Pt2–P5	2.3373(13)	P1–O1	1.566(3)	P4–O10	1.626(4)	Pt2–P4	2.3163(15)	P2–O4	1.583(4)	P4–O8	1.618(4)
Pt2–P6	2.3241(11)	P2–O4	1.547(4)	P5–O19	1.624(4)	Pt2–P8	2.3267(14)	P3–O7	1.570(4)	P5–O13	1.623(4)
Pt2–P7	2.3174(13)	P3–O6	1.587(3)	P6–O20	1.632(4)	Pt2–P6	2.3363(14)	P4–O9	1.532(4)	P6–O13	1.652(4)
Pt2–P8	2.3139(11)	P4–O7	1.578(3)	P7–O19	1.635(4)			P4–O10	1.577(4)	P7–O18	1.629(4)
		P5–O11	1.584(3)	P8–O20	1.634(4)			P5–O11	1.578(4)	P8–O18	1.640(5)

Discussion

Lattice Change due to Photoirradiation. In order to obtain the precise diffraction data during photoirradiation, only the crystals without solvent molecules (except Bzdmp) were selected, because the solvent molecules may be eliminated from the crystal during photoirradiation. Since an alkyl chain has a disordered structure in the Pn2 crystal, only the Pn1 crystal was used for photoirradiation, since the thermal energy emitted from the excited molecules may affect the disordered structure. Therefore, the five crystals of Bu1, Pn1, Bzte1, Bztbu, and Bzdmp among the eight crystals were used for the experiment of photo excitation.

Figure 12 shows the powder diffraction pattern of the Pn1 complex at the light-off and light-on stages. The diffraction peaks of the light-on pattern shift to the higher angles than those at the light-off stage. The shifted pattern, of course, returned to the original one at the light-off stage. This indicates that the unit cell contracts at the excited state. The diffraction pattern should shift to the shorter diffraction angles if the crys-

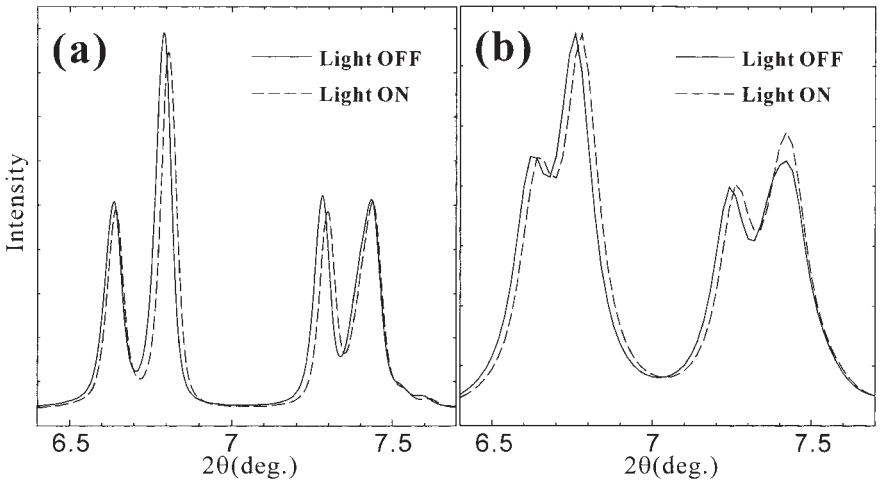

Fig. 12. (a) The powder diffraction patterns of the Pn1 complex at the light-off and light-on stages, measured at the BL02B2 beam line of SPring-8. (b) The plots of the calculated diffraction angles based on the unit-cell dimensions of the single crystals at the light-off and light-on stages.

Table 5. Change of the Unit-Cell Volume (Å^3) at Light-Off (V_{off}) and Light-On (V_{on}) Stages for the Bu1, Pn1, Bzte1, Bztbu, and Bzdmp Crystals

	V_{off}/Å^3	V_{on}/Å^3	$\Delta(V_{on} - V_{off})$	$\Delta\lvert V_{on} - V_{off}\rvert/V_{off}$ (%)
Bu1	1320.18(3)	1312.16(5)	−8.02(4)	0.61
Pn1	3046.45(7)	3026.12(17)	−20.33(12)	0.67
Bzte1	2108.78(12)	2094.92(11)	−13.86(11)	0.66
Bztbu	2696.42(16)	2691.27(12)	−5.15(14)	0.19
Bzdmp	3613.30(6)	3607.44(6)	−5.86(6)	0.16

tal is expanded thermally due to photoirradiation. It is adequate to assume that the excited-state Pt complex becomes smaller than that at the ground state, because there are no other substances which contract on exposure to the Xe lamp. Moreover, it must be emphasized that the diffraction peaks at the light-on stage are sharp and that they indicate no mixing of the original diffraction peaks. This suggests that the photo-excited molecules and the ground-state molecules reached the equilibrium state after a short period and the new crystalline-lattice corresponding to the equilibrium state was produced. The plots in the diffraction patterns of Fig. 12 indicate the calculated diffraction angles based on the unit-cell dimensions at the light-off and light-on stages. It is clear that both of the photo-produced structures at the equilibrium state for the powdered crystals and the single crystal are equivalent, since the unit-cell of the powdered crystals at the light-on stage is the same as the corresponding one of the single crystal. This also indicates that the equilibrium structure is independent of the intensity of incident light or number of incident photons if a sufficient number of photons is exposed to the sample.

The unit-cell dimensions of the five crystals at the light-off and light-on stages are listed in Table 2. Table 5 summarizes the volume changes of the five crystals. The ratio of the volume change, $\Delta|V_{on} - V_{off}|/V_{off}$, is more than 0.6% for the crystals other than Bztbu and Bzdmp.

Structural Change due to Photoirradiation. The intensity data for the five crystals at the light-on stage were collected at 173 K for Bu1, Pn1, and Bzdmp and at 103 K for Bzte1 and Bztbu and the structures were determined by X-ray analyses. In each crystal, there are no significant structural differences in the cation molecules between the light-off and light-on stages. On the other hand, the bond distances in the Pt complex anions are significantly changed from the corresponding ones at light-off stage. We can safely claim that the Pt complex has the D_{4h} $(4/m)$ symmetry except for the exocyclic P=O or P–OH groups. Table 6 shows the averaged Pt–Pt, Pt–P and P–O(–P) bond distances assuming the D_{4h} symmetry. The Pt–Pt and Pt–P bond distances become significantly shorter at light-on stage than those at light-off stage. The changes of the other bond distances are within the experimental error. The shortening of the Pt–Pt and Pt–P bonds are in the range of 0.0019(2) to 0.0127(5) Å and 0.0019(12) to 0.0085(14) Å, respectively. Such differences are probably caused by the different concentrations of the excited molecules in each crystal. The differences in transmittance of the incident light and in the packing around the Pt complex may be responsible for the different concentrations of the excited molecules. It is noticeable that the average Pt–Pt and Pt–P shortenings, $|\Delta(\text{Pt–Pt})|$ and $|\Delta(\text{Pt–P})|$, of two Pt complexes in Pn1 and Bzte1 are 0.0081(3) and 0.0053(11) Å, and 0.0127(5) and 0.0085(14) Å, respectively. The ratios of $|\Delta(\text{Pt–Pt})|$ to $|\Delta(\text{Pt–P})|$ in Pn1 and Bzte1, 1.53 and 1.49, are very close to each other. This suggests that the excited Pt complex anion should have the same structure in each crystal, although the concentrations of the excited molecules may be different among the five crystals. The change at the excited stage is schematically drawn in Fig. 13.

Comparison with the Other Methods. The complex anion of $[Pt_2(pop)_4]^{4-}$ has a strong singlet absorption band associated

Table 6. Averaged Bond Distances (Å) of Pt–Pt, Pt–P, P–O(–P), P=O, and P–O(–H) at Light-Off (D_{off}) and Light-On (D_{on}) Stages and Their Difference (ΔD)

	D_{off}	D_{on}	ΔD		D_{off}	D_{on}	ΔD
Bu1				Bztbu			
Pt–Pt	2.9419(3)	2.9381(3)	−0.0038(3)	Pt–Pt	2.9394(3)	2.9363(4)	−0.0031(3)
Pt–P	2.3338(10)	2.3269(10)	−0.0069(10)	Pt–P	2.3254(12)	2.3235(12)	−0.0019(12)
P–O(–P)	1.632(3)	1.629(3)	−0.003(3)	P–O(–P)	1.630(4)	1.628(4)	−0.002(4)
P=O	1.535(3)	1.530(3)	−0.005(3)	P=O	1.527(4)	1.521(4)	−0.006(4)
P–O(–H)	1.563(3)	1.561(3)	−0.002(3)	P–O(–H)	1.562(3)	1.563(4)	0.001(4)
Pn1				Bzdmp			
Pt–Pt	2.9546(3)	2.9465(3)	−0.0081(3)	Pt–Pt	2.9203(2)	2.9184(2)	−0.0019(2)
Pt–P	2.3318(11)	2.3265(11)	−0.0053(11)	Pt–P	2.3360(8)	2.3327(9)	−0.0033(8)
P–O(–P)	1.630(3)	1.627(4)	−0.003(3)	P–O(–P)	1.638(3)	1.636(3)	−0.002(3)
P=O	1.522(3)	1.518(3)	−0.004(3)	P=O	1.522(3)	1.521(3)	−0.001(3)
P–O(–H)	1.565(3)	1.561(4)	−0.004(4)	P–O(–H)	1.578(3)	1.575(3)	−0.003(3)
Bzte1							
Pt–Pt	2.9726(4)	2.9599(6)	−0.0127(5)				
Pt–P	2.3374(13)	2.3289(14)	−0.0085(14)				
P–O(–P)	1.639(4)	1.628(6)	−0.011(5)				
P=O	1.538(4)	1.532(6)	−0.006(5)				
P–O(–H)	1.558(4)	1.553(5)	−0.005(5)				

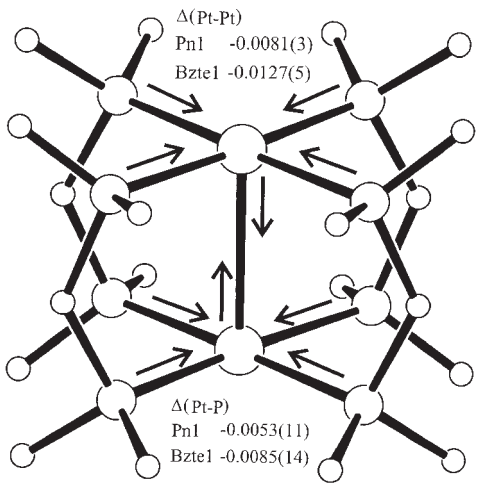

Fig. 13. A schematic drawing of the structural change of the Pt complex anion at the excited state.

with a weakly luminescent state, $^1A_{2u} \leftarrow {}^1A_{1g}$ ($d\sigma^* \rightarrow p\sigma$), which can populate a strongly emissive long-lived triplet state, $^3A_{2u}$ ($d\sigma^* \rightarrow p\sigma$), that can undergo many different chemical reactions. A number of studies have been carried out to elucidate the spectroscopy, photophysics, and photochemistry associated with the excited electronic states of $[Pt_2(pop)_4]^{4-}$ in the 300–450 nm region. It was found from the vibronically resolved absorption and emission spectra of low-temperature crystalline samples of $[N(C_4H_9)_4]_4[Pt_2(pop)_4]$ that the Pt–Pt bond distance for the $^3A_{2u}$ state becomes shorter by about 0.21 Å than the $^1A_{1g}$ ground state. The similarity of the bandwidths and excited state vibrational wavenumbers for the $^1A_{2u}$ and $^3A_{2u}$ states suggest that they have almost the same structure.[21,22] From the combination of the EXAFS method with rapid-flow laser spectroscopy in an aqueous solution with glycerol, it was estimated that the $^3A_{2u}$ state with a lifetime of about 4 μs undergoes a contraction in the Pt–Pt distance of 0.52 ± 0.13 Å and in the Pt–P distance of 0.047 ± 0.011 Å relative to the $^1A_{1g}$ ground state.[23] It was recently reported from a resonance Raman intensity analysis of the $^1A_{2u} \leftarrow {}^1A_{1g}$ transition of $[N(C_4H_9)_4]_4[Pt_2(pop)_4]$ in acetonitrile solution at room temperature that the Pt–Pt bond distance contraction was about 0.225 Å in the initially excited $^1A_{2u}$ state relative to the $^1A_{1g}$ ground state.[24]

The ground and excited states of the $[Pt_2(pop)_4]^{4-}$ anion were investigated using density functional theory.[25] Calculations with different functionals employing quasi-relativistic Pauli and ZORA formalisms predict a Pt–Pt shortening of 0.18–0.51 Å and a Pt–P lengthening of 0.01–0.05 Å.

Coppens et al. have used the time-resolved stroboscopic diffraction technique to observe the structure of $[N(C_2H_5)_4]_3[Pt_2(pop)_3(popH)]$ at the excited state.[13] The frequency and width of the X-ray pulse were 5100 Hz and 33 μs. The laser pulses from a triplet Nd/YAG pump laser ($\lambda = 355$ nm) are synchronized with the X-ray pulses. This means that the intensity data were collected within 33 μs just after the photoirradiation. The data collection was repeated in a time interval of 196 μs and the corresponding intensity data of each time-interval were summarized. The intensity data at the light-off and light-on stages were collected at 17 K and the two sets of data were scaled. Analyzing the structural change using the difference intensities, the Pt–Pt bond shortening was obtained to be 0.28(9) Å and the population of the excited state was 2.0%.

Recently we reported the preliminary structure analyses of the excited state of the Bu1 crystal using the continuous light. The crystal was mounted on a new low-temperature vacuum (LTV) X-ray camera installed at the BL02B1 at SPring-8.[15] The crystal was irradiated with a CW He–Cd blue laser ($\lambda = 442$ nm). The intensity data at the light-off and light-on stages were recorded on the same imaging plate at 54 K. Analyzing the structural change using the difference intensities, the Pt–Pt bond shortening was obtained to be 0.23(4) Å and the

population of the excited state was 1.4(2)%. For the Pn1 complex, the intensity data at the light-off and light-on stages were collected at 123, 173, and 223 K using R-AXIS RAPID. The unit-cell volume contraction and the Pt–Pt distance shortening were observed to be 11 Å^3 and 0.01 Å, respectively, at 173 K.[16]

All the above results suggest that the Pt–Pt bond distances become shorter by 0.2–0.3 Å and the Pt–P bond may contract by 0.1–0.2 Å, although the theoretical calculation indicated a slight lengthening of the Pt–P bond. Considering from the observed bond shortenings of Pt–Pt and Pt–P distances, the concentrations of the excited molecules may be 4–5% in the Pn1 and Bzte1 crystals and 1–2% in the Bu1, Bztbu, and Bzdmp crystals at the light-on stage. If we can assume that the occupancy factor of the excited molecule in Bu1 is the same as that obtained at SPring-8, 1.4%, the bond shortenings for Pt–Pt and Pt–P at the excited state are estimated to be 0.27 and 0.49 Å, respectively. This assumption is adequate because the change of the powdered pattern at the excited state observed at SPring-8 is well explained with the unit-cell change of the single crystal. However, it is probable that the excited molecule in the solid state will take the different structure from that in the gas state or in vacuo, since the excited structure in the solid state should suffer from steric repulsion due to the strong intermolecular interaction. This indicates that the concentration of the excited molecules may be larger than the 4–5% obtained in the above estimation. It seems important to estimate the concentration of the excited molecules before the atomic parameters and the occupancy factors of the model including the ground- and excited-state molecules are refined in the least-squares calculation.

Concluding Remarks

Four crystals with $[Pt_2(pop)_2(popH)_2]^{2-}$ as an anion and tetrabutyl-, tetrapentyl-, benzyltriethyl-, or benzyltributylammonium as a cation and one crystal with $[Pt_2(pop)_4]^{4-}$ as an anion and benzyldimethylphenylammonium as a cation were prepared. Their crystal structures containing the different crystal forms were determined by X-ray analyses. When each crystal was irradiated with a xenon lamp, the photo-excited molecules and the ground-state molecules reached an equilibrium state after a short period and the new crystalline-lattice corresponding to the equilibrium state was produced. The unit-cell dimensions significantly contracted due to the formation of the equilibrium state. The intensity data of each crystal at light-on and light-off stages were collected and the structures were analyzed by using X-rays at 173 or 103 K. The Pt–Pt and Pt–P bond distances are significantly shortened at light-on stage. The bond shortenings of the equilibrium state should come from the structure of the excited molecule. If one starts from the bond shortenings of Pt–Pt and Pt–P distances at the excited state obtained by the spectroscopic data or theoretical calculation, the concentrations of the excited molecules may be 4–5% in the Pn1 and Bzte1 crystals and 1–2% in the Bu1, Bztbu, and Bzdmp crystals at the light-on stage if one assumes the excited structure in the solid state is not heavily distorted due to intermolecular interactions. The Pt–Pt shortening, 0.27 Å, is in good agreement with the corresponding one obtained at SPring-8, 0.23 Å, and the value observed by the stroboscopic method, 0.28 Å.

This work was supported financially by CREST from JST. The powder diffraction experiment at BL02B2 of SPring-8 were performed with the approval of JASRI (Proposal No. 2002B0329-ND1-np). We thank Dr. Ken-ichi Kato of JASRI for his technical support.

References

1 a) Y. Ohashi, *Acc. Chem. Res.*, **21**, 268 (1988). b) T. Nemoto and Y. Ohashi, *Bull. Chem. Soc. Jpn.*, **72**, 1971 (1999).

2 a) T. Koura and Y. Ohashi, *Bull. Chem. Soc. Jpn.*, **70**, 2417 (1997). b) T. Ohhara, H. Uekusa, Y. Ohashi, I. Tanaka, S. Kumazawa, and N. Niimura, *Acta Crystallogr.*, **B57**, 551 (2001).

3 T. Hosoya, T. Ohhara, H. Uekusa, and Y. Ohashi, *Bull. Chem. Soc. Jpn.*, **75**, 2147 (2002).

4 N. Tokitoh, Y. Arai, T. Sasamori, R. Okazaki, S. Nagase, H. Uekusa, and Y. Ohashi, *J. Am. Chem. Soc.*, **120**, 433 (1998).

5 Y. Ohashi, Y. Sakai, A. Sekine, Y. Arai, Y. Ohgo, N. Kamiya, and H. Iwasaki, *Bull. Chem. Soc. Jpn.*, **68**, 2517 (1995).

6 a) J. Harada, H. Uekusa, and Y. Ohashi, *J. Am. Chem. Soc.*, **121**, 5809 (1999). b) P. Naumov, A. Sekine, H. Uekusa, and Y. Ohashi, *J. Am. Chem. Soc.*, **124**, 8540 (2002).

7 M. Kawano, A. Ishikawa, Y. Morioka, H. Tomizawa, E. Miki, and Y. Ohashi, *J. Chem. Soc., Dalton Trans.*, **2000**, 2425.

8 M. Kawano, T. Sano, J. Abe, and Y. Ohashi, *J. Am. Chem. Soc.*, **121**, 8106 (1999).

9 M. Kawano, K. Hirai, H. Tomioka, and Y. Ohashi, *J. Am. Chem. Soc.*, **123**, 6904 (2001).

10 a) T. Takayama, M. Kawano, H. Uekusa, Y. Ohashi, and T. Sugawara, *Helv. Chim. Acta*, **86**, 1352 (2003). b) M. Kawano, T. Takayama, H. Uekusa, Y. Ohashi, Y. Ozawa, K. Matsubara, H. Imabayashi, M. Mitsumi, and K. Toriumi, *Chem. Lett.*, **32**, 922 (2003).

11 S. Techert, F. Schotte, and M. Wulff, *Phys. Rev. Lett.*, **86**, 2030 (2001).

12 K. Moffat, *Chem. Rev.*, **101**, 1569 (2001).

13 C. D. Kim, S. Pillet, G. Wu, W. K. Fullagar, and P. Coppens, *Acta Crystallogr.*, **A58**, 133 (2002).

14 T. Ikagawa, T. Okumura, T. Otsuka, and Y. Kaizu, *Chem. Lett.*, **1997**, 829.

15 Y. Ozawa, M. Terashima, M. Mitsumi, K. Toriumi, N. Yasuda, H. Uekusa, and Y. Ohashi, *Chem. Lett.*, **32**, 62 (2003).

16 N. Yasuda, M. Kanazawa, H. Uekusa, and Y. Ohashi, *Chem. Lett.*, **2002**, 1132.

17 C.-M. Che, L. G. Butler, P. J. Grunthaner, and B. Gray, *Inorg. Chem.*, **24**, 4662 (1985).

18 A. P. Zipp, *Coord. Chem. Rev.*, **84**, 47 (1988).

19 G. M. Sheldrick, "SHELXS97, a program for the solution of crystal structures," University of Göttingen, Germany (1997).

20 G. M. Sheldrick, "SHELXL97, a program for the refinement of crystal structures," University of Göttingen, Germany (1997).

21 S. F. Rice and H. B. Gray, *J. Am. Chem. Soc.*, **105**, 4571 (1983).

22 A. E. Stiegman, S. F. Rice, H. B. Gray, and V. M. Miskowski, *Inorg. Chem.*, **26**, 1112 (1987).

23 D. J. Thiel, P. Livins, E. A. Stern, and A. Lewis, *Nature*, **362**, 40 (1993).

24 K. H. Leung, D. L. Phillips, C.-M. Che, and V. M. Miskowski, *J. Raman Spectrosc.*, **30**, 987 (1999).

25 I. V. Novozhilova, A. V. Volkov, and P. Coppens, *J. Am. Chem. Soc.*, **125**, 1079 (2003).